Available online at www.sciencedirect.com
ScienceDirect
Polymer 48 (2007) 7201–7210
polymer
www.elsevier.com/locate/polymer

Morphology of semicrystalline oxyethylene/oxybutylene block copolymer thin films on mica

Guo-Dong Liang [a], Jun-Ting Xu [a,b,*], Zhi-Qiang Fan [a,b], Shao-Min Mai [c], Anthony J. Ryan [c]

[a] *Key Laboratory of Macromolecular Synthesis and Functionalization, Department of Polymer Science and Engineering, Zhejiang University, 38 Zheda Road, Hangzhou 310027, China*
[b] *State Key Laboratory of Chemical Engineering, College of Materials and Chemical Engineering, Zhejiang University, Hangzhou 310027, China*
[c] *Department of Chemistry, The University of Sheffield, S3 7HF Sheffield, UK*

Received 5 April 2007; received in revised form 24 September 2007; accepted 26 September 2007
Available online 5 October 2007

Abstract

The morphology of as-cast and annealed thin films of four symmetric semicrystalline block copolymers on mica was investigated by tapping mode atomic force microscopy (AFM) and grazing incidence X-ray diffraction (XRD). It is found that the morphology of the thin films is dependent on chain length of oxyethylene/oxybutylene block copolymers. The as-cast thin films of the shorter E_mB_n block copolymers on mica exhibit a multi-layered lamellar structure parallel to the surface, in which the stems of the E crystals in the first half polymer layer contacting mica are parallel to the mica surface and perpendicular to the mica surface in the upper polymer layers. In contrast, the as-cast thin film of longer $E_{224}B_{114}$ exhibits a structure with mixed orientations of lamellar microdomains on a half polymer layer parallel to the surface. After annealing, the multi-layered structure on mica is transformed into a half-layered, densely branched structure, which is formed following a diffusion-limited aggregation mechanism, opposed to the featureless half-layered structure on silicon. Upon annealing, the upper polymer layers gradually retreat and the remaining area becomes thicker, but in contrast the first half polymer layer contacting mica becomes thinner due to wetting and the parallel orientation of the E crystal stems. The densely branched structure and the different chain orientations of the E crystal stems in the first half polymer layer contacting mica are attributed to the strong interaction between the E block and mica, as revealed by our previous work. The width of branches was employed to analyze the kinetics of secondary crystallization. It is also found that the width of the branches and the velocity of crystal front decrease as the chain length increases.

Keywords: Thin film; Block copolymer; Crystallization

1. Introduction

Block copolymer thin films attract increasing attention due to their ability to self-assemble into a plethora of patterns, which are dependent on components and composition of the block copolymers, boundary condition and fabrication process [1–36]. The morphology of block copolymer thin films depends on many factors, such as polymer structure, surface property, preparation conditions and thermal history. The chain length of block copolymer determines not only the size of microphase-separated domains, but also the segregation strength. The segregation strength plays an important role in the formation of microphase-separated morphology, especially for semicrystalline block copolymer. When the block copolymer contains a crystallizable component, microphase separation will compete or couple with crystallization. It has been revealed in bulk that strong segregation may lead to confined crystallization for a crystalline/rubbery block copolymer, but microphase separation in the melt can be destroyed by crystallization when the segregation strength is weak [37,38]. When microphase separation and crystallization take place simultaneously,

* Corresponding author. Key Laboratory of Macromolecular Synthesis and Functionalization, Department of Polymer Science and Engineering, Zhejiang University, 38 Zheda Road, Hangzhou 310027, China. Tel./fax: +86 571 87952400.
E-mail address: xujt@zju.edu.cn (J.-T. Xu).

0032-3861/$ - see front matter © 2007 Elsevier Ltd. All rights reserved.
doi:10.1016/j.polymer.2007.09.049

there may also be a coupling effect between them [39,40]. Herein we report the effect of segregation strength on thin film morphology of semicrystalline block copolymers. Moreover, the substrate surface is well recognized as a crucial parameter affecting thin film morphology. The effect of surface properties of substrates on self-assembly of block copolymer thin film has been well understood for amorphous block copolymers [41–46]. For semicrystalline block copolymers, however, the situation is more complicated, since there is not only the orientation of block copolymer to consider, but also crystallization processes, such as nucleation and growth, may be influenced by the substrate surface. In our previous work [47], we studied the morphology of multi-layered E_mB_n thin films on mica and found that the strong interaction between the crystalline E block and mica led to the chain orientation of the E crystal stems parallel to the substrate surface in the first half polymer layer contacting mica, which is different from the chain orientation in the other polymer layers, as well as from that in the first half polymer layer on silicon [47]. In this paper, we study the morphology of half-layered E_mB_n thin films on mica so that the effect of interaction between the E block and mica on thin film morphology can be well characterized. For the purpose of comparison, morphology of the as-cast thin films of E_mB_n on mica was also reported.

2. Experimental

2.1. Materials

The synthesis and characterization of oxyethylene/oxybutylene block copolymers, $E_{76}B_{38}$, $E_{114}B_{56}$, $E_{155}B_{76}$ and $E_{224}B_{113}$ (where E and B denote oxyethylene and oxybutylene units, respectively, and denoted as E_mB_n, the subscripts refer to the average degree of polymerization), have been described elsewhere [48–50]. All the block copolymers have narrow molecular weight distributions ($M_w/M_n < 1.05$) determined by GPC and have a lamellar morphology in both the solid and liquid bulk phases. Parameters of the block copolymers are summarized in Table 1.

2.2. Preparation of block copolymer thin films

Block copolymer thin films were prepared by spin-coating E_mB_n block copolymer/dichloromethane solution (0.5 w/v%) on mica. The uppermost layers of mica were cleaved and the block copolymers were spin-coated on the clean and fresh mica surface. Solvent was allowed to evaporate simultaneously during spin-coating process. Annealing of diblock copolymer thin film was conducted at 35 °C for various times under vacuum (10 torr). After annealing of the thin films, AFM experiment was conducted immediately.

Table 1
Parameters of E_mB_n diblock copolymers

Copolymer	ϕ_E[a] (solid state)	w_E[b] (solid state)	Long period in the bulk L_0 (nm)	T_c[c] (°C)	$N\chi$[d]
$E_{76}B_{38}$	0.49	0.55	16.7	35	19.9
$E_{114}B_{56}$	0.50	0.55	19.8	38	29.7
$E_{155}B_{76}$	0.50	0.56	22.0	40	40.4
$E_{224}B_{113}$	0.49	0.55	33.3	43	58.9

[a] $\phi_E = n/[n + (72/44)(1.23/0.97)m]$, ϕ_E: the volume fraction of the E block, 1.23 g/cm^3 being the density of E in the crystalline state and 0.97 g/cm^3 the density of B in the liquid state, both at 20 °C.
[b] $w_E = n/[n + (72/44)m]$, w_E: the weight fraction of the E block.
[c] T_c at cooling rate of 10 °C/min.
[d] χ: calculated for E_nB_m diblock copolymer bulk at 20 °C [50].

2.3. Atomic force microscopy (AFM)

The thin film morphology of E_mB_n block copolymers was investigated by atomic force microscopy (SPA 300HV/SPI3800N Probe Station, Seiko instruments Inc., Japan) in the tapping mode. A silicon micro-cantilever with a spring constant 16 N/m and resonance frequency ~138 kHz was used. The scan rate ranged from 0.5 to 2.0 Hz to optimize the quality of AFM image. The set-point ratio, the ratio between the set-point amplitude and the free vibration amplitude (the lowest amplitude when tip and sample are not in contact), was chosen to be ~0.8. Parameters characterizing the feature of thin film such as thickness of lamellar and difference of phase shift were obtained directly from cross-sectional profiles. In order to ensure the repeatability of the data, cross-sectional profiles from different area of height or phase images were necessary. At least 10 values were obtained for each parameter.

2.4. Grazing incidence X-ray diffraction (GIXRD)

Grazing incidence techniques were carried out to investigate the crystal structure of the block copolymer thin films at room temperature. A BEDE D1 high-resolution X-ray diffractometer equipped with a Cu Kα radiation source was used. The diffracted beam is in the plane defined by the incidence beam and the surface normal. This geometry is sensitive to the structure parallel to the surface. Different grazing incidence angles ranging from 0.2° to 0.8° were tested. The XRD curves were scanned in the 2θ range of 3.0–30°.

3. Results and discussion

3.1. Morphology of the as-cast thin films

Fig. 1 shows the AFM height image and corresponding cross-sectional profile of as-cast $E_{76}B_{38}$ thin film on mica. It is observed that the as-cast $E_{76}B_{38}$ thin film on mica is composed of multiple polymer layers parallel to the mica surface with two series of thickness, L (16 nm and 8.8 nm, respectively), which are close to the long period L_0 (16.7 nm) and $1/2L_0$ of crystallized $E_{76}B_{38}$ in the bulk, respectively [51]. In block copolymer thin films, polymer layers usually exhibit two series of thickness depending on the symmetry of thin films: xL_0 for symmetrical wetting or $(x + 1/2)L_0$ for asymmetrical wetting (where L_0 is the long period of block copolymer in bulk and x is an integer) [4]. When the thickness of the thin film does not meet this condition, films with $x > 1$ form rough surfaces with holes and islands, whereas in films thinner than

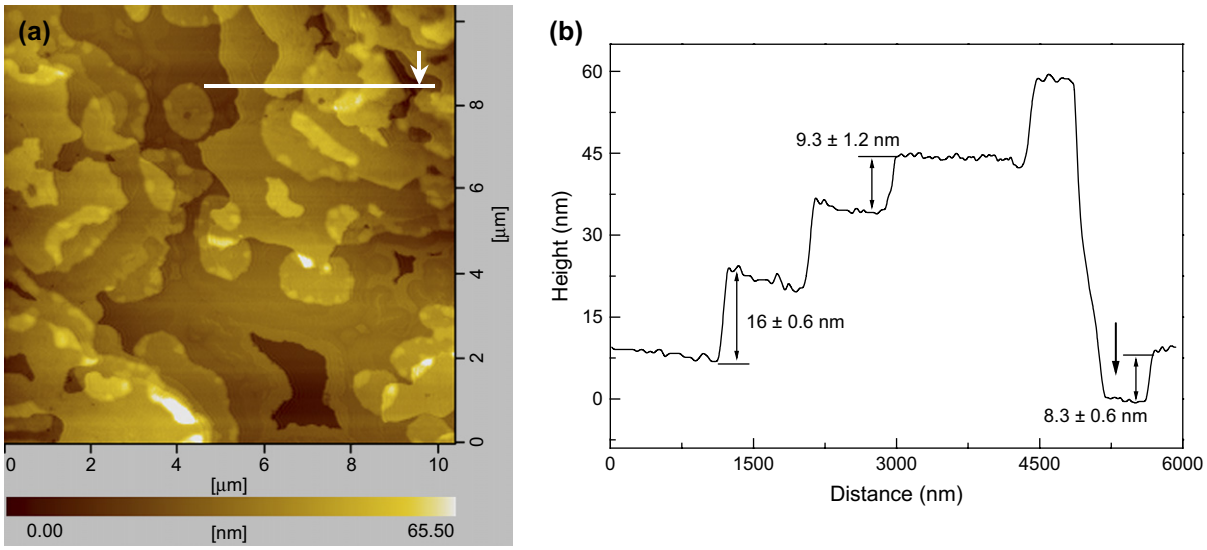

Fig. 1. AFM height image (a) and cross-sectional profile (b) of as-cast $E_{76}B_{38}$ thin film. The arrow indicates the hole throughout the polymer thin film.

$x = 1$, dewetting will take place. In the present work, the hydrophilic E block and hydrophobic B block are located at polymer/mica and polymer/air interfaces, respectively, so the top of the mica surface is a half polymer layer. We also observed some polymer layers with thickness of $L_0/2$ besides the first layer on the substrate. This indicates that the crystalline domains are possibly composed of double crystalline layers somewhere in the as-cast $E_{76}B_{38}$ thin films [52]. The displacement between the two adjacent crystalline layers leads to the polymer layers of the thickness $L_0/2$. However, considering that it is difficult for the polymer chains to reach thermodynamic equilibrium in the as-cast thin films, parts of the E blocks inevitably interconnect the double crystalline layers and somewhere the crystalline domains may be composed of single crystalline layer. The as-cast $E_{114}B_{56}$ and $E_{155}B_{76}$ thin films on mica exhibit a similar structure.

For the as-cast $E_{224}B_{113}$ thin film on mica, the overall morphology is still multi-layered with a half polymer layer contacting the mica surface (Fig. 2a and b) composed of multiple polymer layers parallel to the mica surface with two series of thickness, L (29 nm and 15 nm, respectively), which are close to the long period L_0 (33.3 nm) and $1/2L_0$ of crystallized $E_{224}B_{113}$ in the bulk, respectively. However, we also observe a periodical structure parallel to the surface (Fig. 2a and b), showing that the microphase-separated lamellar microdomains are also perpendicular to the surface at an even closer match to L_0 (33.8 nm). As a result, the morphology of as-cast $E_{224}B_{113}$ thin film comprises lamellar microdomains with mixed orientations (both perpendicular and parallel) on a half polymer layer parallel to the mica surface.

Grazing incidence X-ray diffraction (GIXRD) was used to probe the chain orientation of the crystal stems. Experiments at various incidence angles (a_i) were conducted so that chain orientation in different polymer layers can be determined. At a larger incidence angle X-ray can penetrate thicker polymer layers, while at a smaller incidence angle only chain orientation of polymer crystals in the upper polymer layers can be probed due to the smaller penetration depth of X-ray. Fig. 3 shows the GIXRD curves of the as-cast E_mB_n thin films at $a_i = 0.6°$ and $a_i = 0.2°$. According to the geometry of GIXRD, only structures parallel to the substrate surface can be detected [53–55]. One can see that at $a_i = 0.6°$ the reflection (120) of PEO crystals is observed for the as-cast thin films of all four E_mB_n block copolymers, whereas at $a_i = 0.2°$ the reflection (120) of PEO crystals only appears in the GIXRD curve of as-cast $E_{224}B_{113}$ thin film. The GIXRD result shows that in the as-cast thin films of shorter E_mB_n ($E_{76}B_{38}$, $E_{114}B_{56}$ and $E_{155}B_{76}$) the chain orientation of the E crystal stems in the first half polymer layer contacting mica surface is parallel to the substrate, while in the upper polymer layers the stems of E crystals are perpendicular to the substrate. For the long $E_{224}B_{113}$, there also exist stems of the E crystals parallel to the substrate surface in the upper polymer layers, which is in accordance with AFM observation. The morphology with mixed orientations has also been reported for the thin films of semicrystalline poly(styrene)-*b*-poly(L-lactide) block copolymer [56]. The combination of AFM and GIXRD results leads to a model of the structures of the as-cast thin films of shorter and longer E_mB_n block copolymers shown schematically in Fig. 4.

When compared with the as-cast thin film morphology of E_mB_n on silicon, two differences are noticed. First, the chain orientation of the E crystal stems in the first half polymer layer contacting the substrates has changed. The stems of the E crystals are parallel to the surface of mica, but perpendicular to the surface of silicon. This difference arises from the strong interaction between the surface of mica and the E block. It is well known that mica is a layered silicate and contains different kinds of cations, especially lots of K^+, and the oxygen atoms in the E block coordinate with these cations [57–59], in a manner analogous to the chelation of cations by crown-ethers which are cyclic E_m. This was verified by infrared spectra in

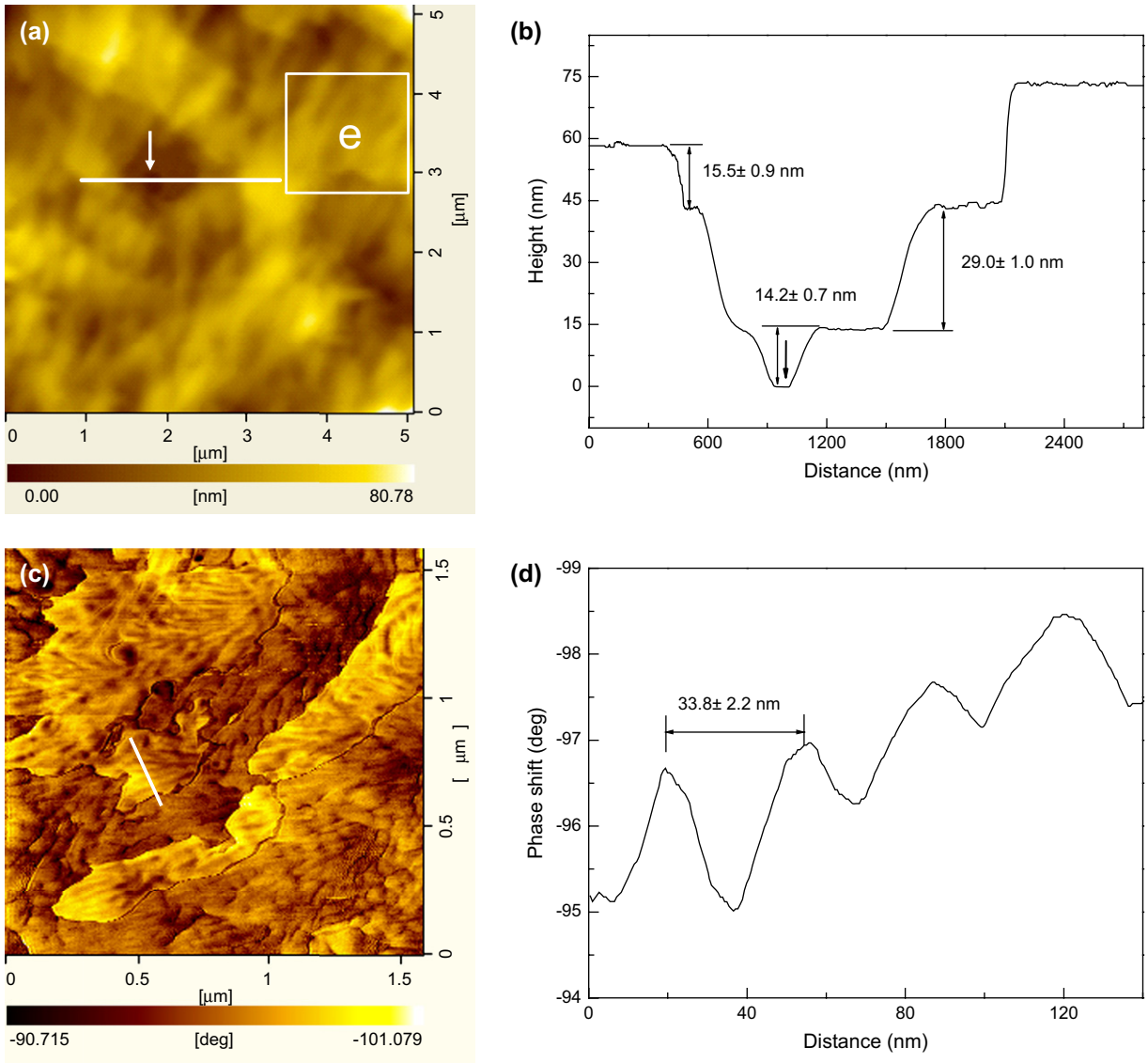

Fig. 2. AFM images and cross-sectional profiles of the as-cast $E_{224}B_{113}$ thin film. (a) Height image; (b) cross-sectional profile along the line in (a); (c) phase image of the white box in (a); (d) cross-sectional profile along the line in (c).

our previous work [47]. Secondly, whilst all of the lamellar microdomains of $E_{224}B_{113}$ are perpendicular to the substrate surface in the thin film on silicon, the lamellar microdomains of the upper polymer layers on mica are only partially perpendicular to the substrate surface. The stems of the E crystal in the first half polymer layer contacting mica and partial stems in the upper polymer layers are still parallel to the mica surface. This is a result of competition between the favorable surface interaction with the E block and microphase separation. The attraction between the E block and the mica surface induces the lamellar microdomains in the first polymer layer to orient parallel to the mica surface and the lamellar microdomains in the upper polymer layers tend to adopt the same orientation to minimize the unfavorable interaction between the E and B blocks. Conversely the high segregation strength tends to orient the lamellar microdomains perpendicular to the mica surface. Therefore, mixed orientations of the lamellar microdomains occur in the upper polymer layers on mica.

3.2. Morphology of the annealed thin films

The AFM images of the annealed E_mB_n thin films are shown in Fig. 5. The height image shows that all the annealed E_mB_n thin films exhibit a densely branched morphology. Such a densely branched morphology is frequently observed in thin films of poly(ethylene oxide) homopolymer [36,60] and its blends [61]. In annealed thin films of E_mB_n the lamellar microdomains orientate parallel to the mica surface, since no periodical structure is observed in the direction parallel to the mica surface. This conclusion is further supported by the observation of a densely branched structure, which is typically formed by adsorption and crystallization. If the lamellar microdomains were perpendicular to the mica surface, the B block would also be located at the mica surface and the densely branched structure could not be formed. The cross-sectional profile reveals that the annealed E_mB_n thin films comprise single half polymer layer. This shows that morphological

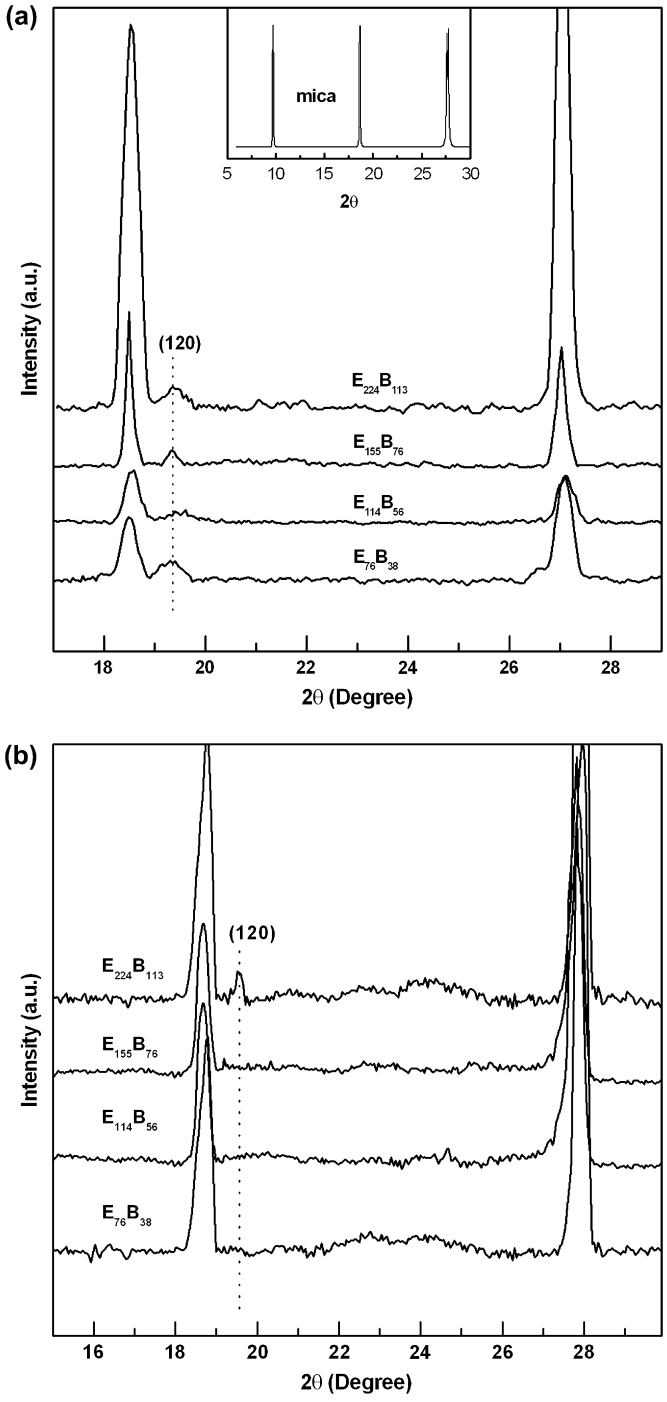

Fig. 3. Grazing incidence X-ray diffraction curves of the as-cast E_mB_n thin films on mica at incident angles $a_i = 0.6°$ (a) and $a_i = 0.2°$ (b).

transformation from a multi-layered structure into a half-layered lamellar structure occurs for all E_mB_n block copolymers during annealing. This process involves mass transport between the different layers. It should be noted that the E domain in the first half layer and the E domain in the upper layer are spaced by an amorphous poly(oxybutylene) domain, which is formed by microphase separation. This indicates that the secondary crystallization of the E block during annealing overcomes microphase separation and dominates re-organization

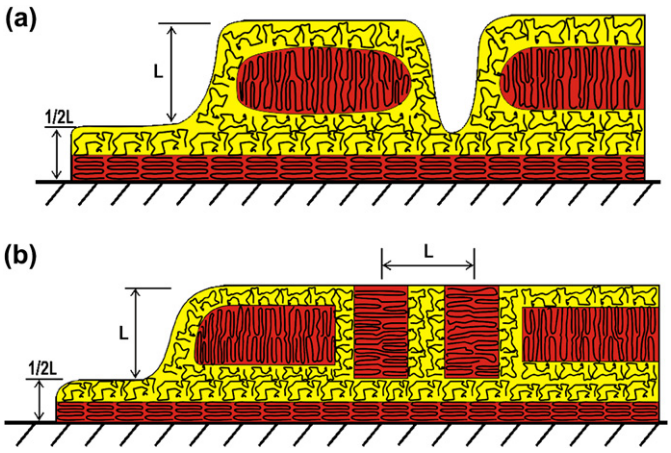

Fig. 4. Schematic structures of the as-cast $E_{76}B_{38}$ (a) and $E_{224}B_{113}$ (b) thin films on mica.

of thin films. Fig. 6 shows the GIXRD curves of the annealed E_mB_n thin films on mica. One can see that even at $a_i = 0.2°$ the (120) reflections are observed for all E_mB_n thin films, showing that the stems of the E crystals in the half-layered polymer thin films on mica are still parallel to the mica surface.

In contrast to the half-layered and densely branched morphology of the annealed E_mB_n thin films on mica, multi-layered structure is formed for shorter E_mB_n block copolymer thin films on silicon and spherulite morphology is formed for the annealed $E_{224}B_{113}$ thin film on silicon [52]. It should be noted that the thin films of E_mB_n block copolymers on mica and on silicon are prepared under the same conditions. The formation of half-layered polymer thin film on mica but multi-layered structure on silicon shows that the wetting of E_mB_n block copolymers on mica is more favorable, thus the polymers on the upper layer migrate completely to the first half layer. When thin films of the shorter E_mB_n block copolymers ($E_{76}B_{38}$, $E_{114}B_{56}$, $E_{155}B_{76}$) on silicon are prepared at a lower concentration (0.1 wt/v%), featureless half-layered structure is formed for annealed thin films, as shown in Fig. 7. The densely branched structure of E_mB_n ultra-thin films is typically formed via a diffusion-limited aggregation (DLA) mechanism [62,63]. During secondary crystallization of E_mB_n thin films, the E crystals grow by attaching the macromolecules diffusing towards the edge of crystal. When crystallization rate is faster than the diffusion rate, depletion zones may be produced at the frontiers of crystallization and the densely branched structure is formed. That no densely branched structure is formed for the E_mB_n block thin films on silicon indicates that the diffusion rate of E_mB_n is larger than the crystallization rate at the same crystallization conditions. Obviously the strong interaction between the E blocks and mica may be responsible for the slower diffusion rate of E_mB_n on mica.

3.3. Morphological transformation upon annealing

Fig. 8 shows that the AFM images of $E_{224}B_{113}$ thin film annealed at 35 °C for various times. One can see from Fig. 8 that

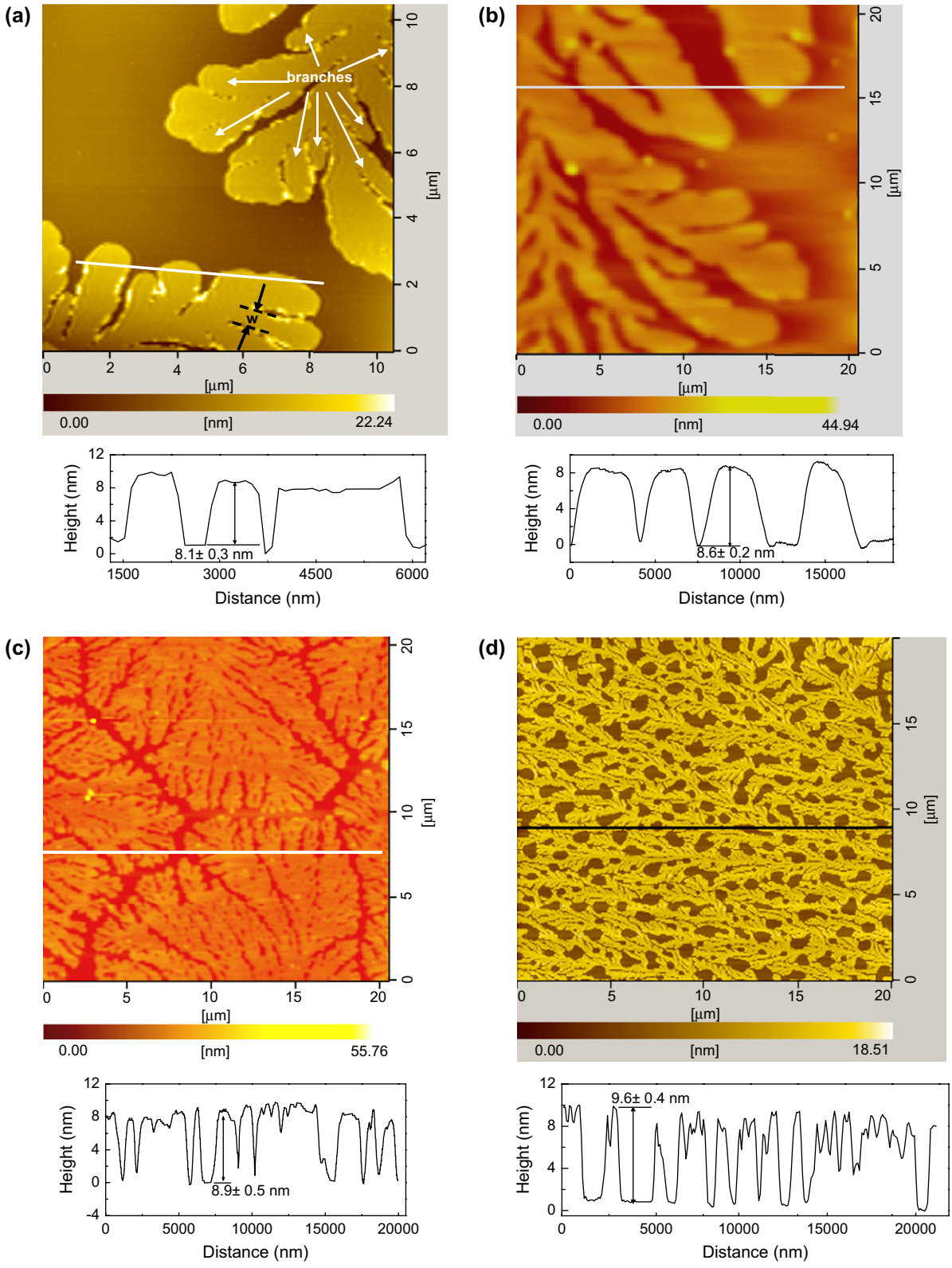

Fig. 5. AFM height images of annealed E_mB_n thin films spin-coated on mica from solution at concentration of 0.5 wt/v% after annealing at 35 °C for 30 h. (a) $E_{76}B_{38}$; (b) $E_{114}B_{56}$; (c) $E_{155}B_{76}$; (d) $E_{224}B_{113}$.

a process akin to dewetting occurs for the upper polymer layers upon annealing. As annealing progresses, polymers in the upper layers become fewer and fewer and finally they disappear. This shows that the polymers at the upper layers migrate to the first half polymer layer contacting the mica surface during annealing, increasing the total area of coverage. Furthermore cracks also appear in the first half polymer layer upon annealing and these cracks become larger with progress

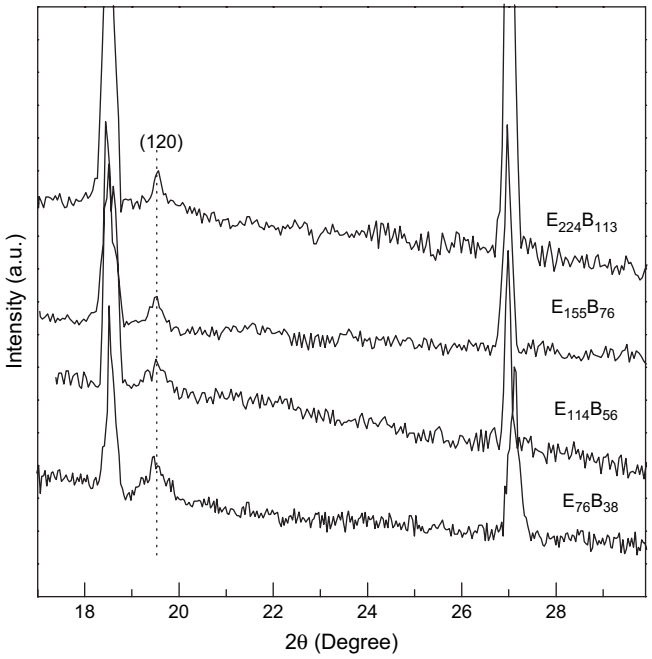

Fig. 6. Grazing incidence X-ray diffraction curves of the annealed E_mB_n thin films on mica at incident angle $a_i = 0.2°$.

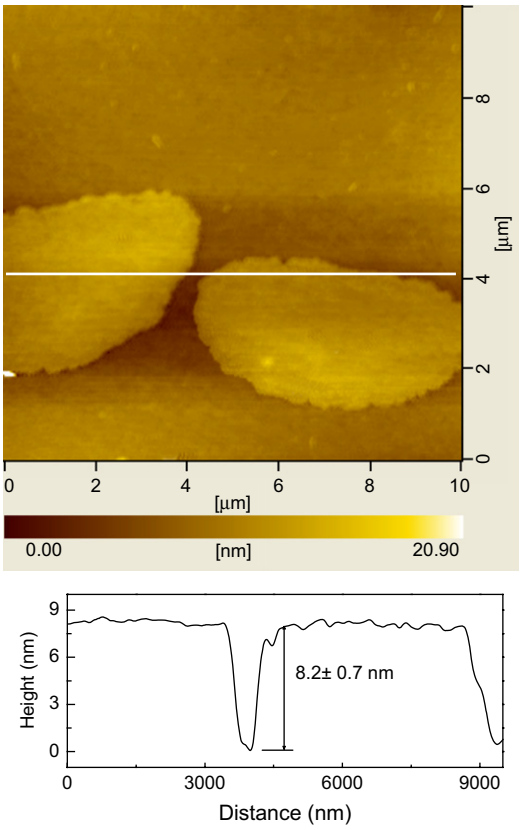

Fig. 7. AFM height image of half-layered $E_{76}B_{38}$ thin film on silicon prepared at a lower concentration (0.1 wt/v%).

of annealing and there is a corresponding decrease in the thickness of the first half polymer during annealing. Based on the conservation of mass, the only explanation for this phenomenon is that the first half polymer layer spreads on the mica surface during annealing. This is understandable, since there exists a favorable interaction between the E block with mica and wetting will take place upon annealing. The variations of the thicknesses of the first half layer and the upper layer with annealing time are illustrated in Figs. 9 and 10, respectively. One can see from Fig. 9 that the thickness of the first half polymer layer decreases gradually during annealing. Such a trend is more evident for the longer block copolymer. In contrast, the thickness of upper polymer layer increases with annealing time and there is a larger increase in the thickness for the longer block copolymers (Fig. 10). Annealing usually leads to increase in crystallinity and the long period of the lamellar microdomains becomes larger accordingly. In the upper polymer layers, the stems of the E crystals are perpendicular to the mica surface and the lamellar microdomains are parallel to the mica surface and thus the increase in thin film thickness reflects the increase of long period. In the first half polymer layer contacting mica, since both the stems of the E crystals and the lamellar microdomains are parallel to the mica surface, annealing and dewetting lead to thinning of this half polymer layer.

3.4. Kinetics of secondary crystallization

Since annealing leads to morphological transformation from multi-layered structure into half-layered densely branched structure, secondary crystallization takes place upon annealing. The width of branches formed upon annealing can be used to analyze kinetics of secondary crystallization. Comparing the annealed thin films of different E_mB_n block copolymers, one can see that the width of the branches decreases as the chain length increases, as shown in Fig. 11.

Crystals constrained into thin films grow by attaching molecules arriving at the edge of the crystals by diffusion. If the probability for desorption from the crystals is low, the molecules will attach to points at the crystal frontier, where they arrive first, and eventually the densely branched or fractal patterns are formed. Here, we will focus on the width of the fingers. To ensure the reliability of the analysis, only the well-developed fingers with constant width over a large distance are statistically analyzed.

The probability that a molecule detaches from (P_d) or rests at (P_r) the crystals can be expressed as [64]:

$$P_d \sim \exp(-\Delta f_m/k_B T) \sim \exp\left(-\Delta T \Delta h_m/k_B T_m^0 T\right) \quad (1)$$

$$P_r = 1 - P_d \quad (2)$$

where Δf_m and Δh_m are the free energy and the heat of fusion per unit volume, respectively. ΔT is the difference between the equilibrium melting temperature T_m^0 and the crystallization temperature T and k_B is Boltzmann constant.

$$d^2 \sim f D_s \tau_a \sim f D_s \tau_c/\left(1 - P_d\right) \sim f D_s \tau_c/P_r \sim f D_s \tau_c/ [1 - \exp(-C_1 \Delta T/T)] \quad (3)$$

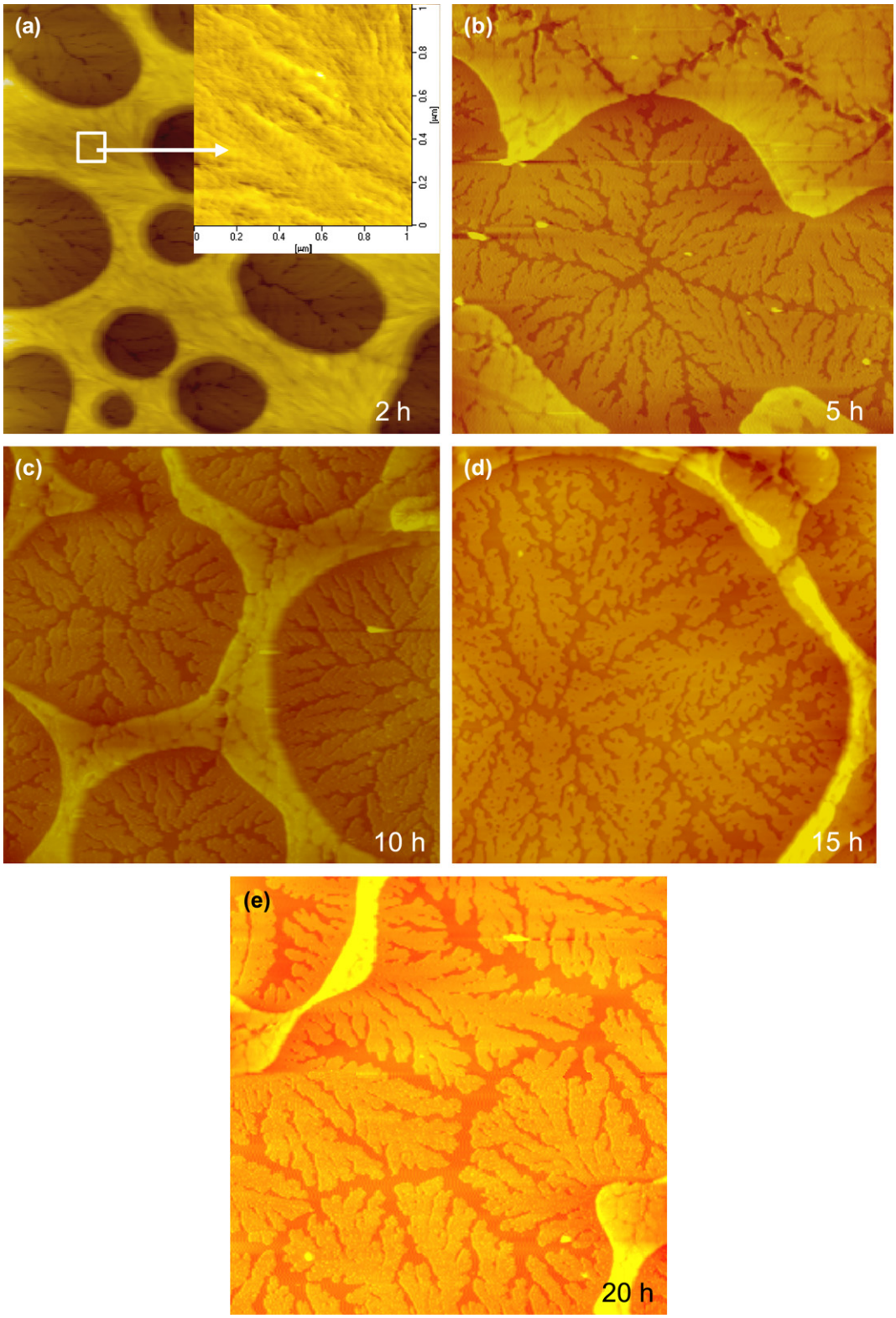

Fig. 8. AFM height images of $E_{224}B_{113}$ thin film on mica at various annealing times.

where d is the width of the depleted zone. D_s and τ_a are the diffusion coefficient and the average time a polymer needs to get attached to the crystal. f is the accumulation factor, the ratio of surface occupied by the adsorbed and a crystallized molecule. $C_1 = \Delta h_m/k_B T_m$ and τ_c is the characteristic time for a molecule to move from one site to its neighboring site. The velocity of the crystal front, υ, can be expressed as [65,66]:

$$\upsilon \sim (D_s/f\tau_a)^{1/2} \tag{4}$$

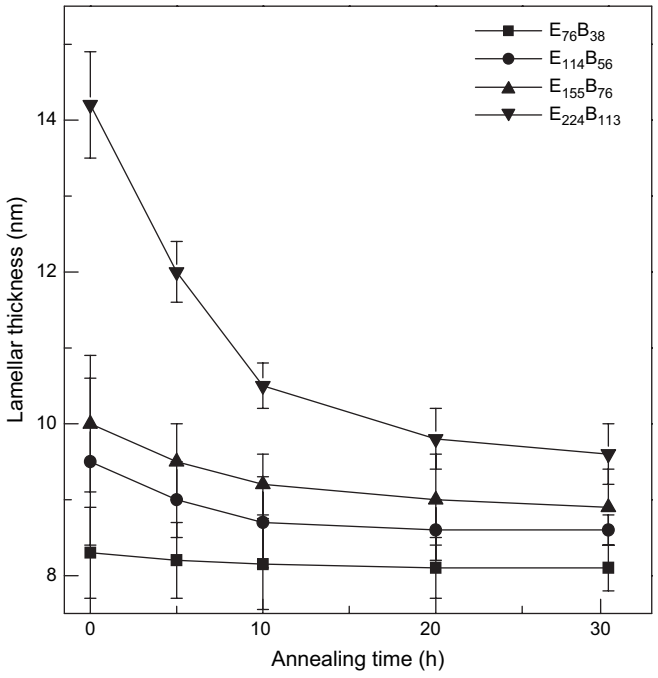

Fig. 9. Variation of the thickness of the first half polymer layer contacting the surface upon annealing for the E_mB_n thin films on mica.

Thus the width of the depleted zone d can be related to D_s and v.

$$d \sim D_s/v \tag{5}$$

There exists positive linear relation between the average width of the fingers w and d.

So one can obtain:

$$w \sim D_s/v \tag{6}$$

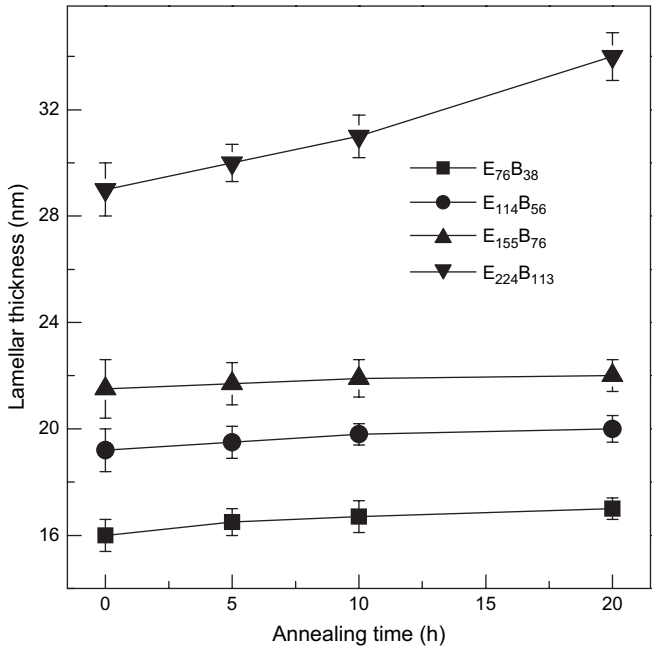

Fig. 10. Variation of the thickness of the upper polymer layer upon annealing for the E_mB_n thin films on mica.

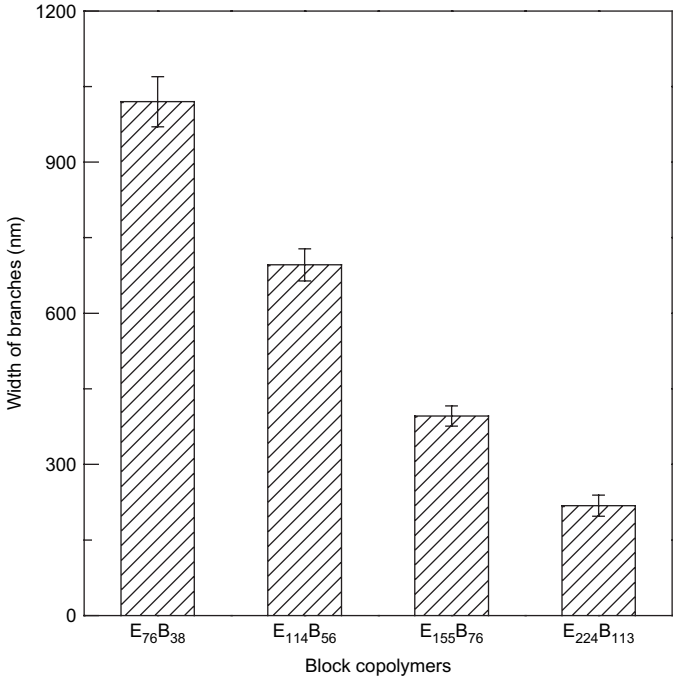

Fig. 11. Width of branches for different E_mB_n thin films after annealing for 30 h.

Table 2
Values of wM^2 for E_nB_m block copolymer thin films

Sample	w[a] (nm)	M (g/mol)	$wM^2 \times 10^{-4}$
$E_{76}B_{38}$	1020 ± 50	6082	3.77
$E_{114}B_{56}$	696 ± 32	9050	5.70
$E_{155}B_{76}$	396 ± 20	12,294	5.98
$E_{224}B_{113}$	218 ± 21	17,994	7.06

[a] Width of branches w is measured directly from cross-sectional profile of every annealed thin film. To make sure the creditability of analysis, only the well-developed branches with constant width over a large distance are used for statistics. At least 10 values at different areas are required to determine its average value.

If we estimate the diffusion coefficient D_s to go with $D_s \sim M^{-2}$ [67], we obtain:

$$wM^2 \sim 1/v \tag{7}$$

The values of wM^2 for E_mB_n diblock copolymer thin films after annealing are summarized in Table 2. It is found that the values of wM^2 increase with the increase of the chain length. The value of wM^2 for $E_{224}B_{113}$ is nearly twice that for $E_{76}B_{38}$, indicating that the velocity of crystal front for $E_{224}B_{113}$ thin film is only half of that for $E_{76}B_{38}$ thin film.

4. Conclusion

The as-cast thin films of shorter E_mB_n ($E_{76}B_{38}$, $E_{114}B_{56}$ and $E_{155}B_{76}$) on mica exhibit a multi-layered structure with lamellar microdomains parallel to the surface. In the as-cast thin film of the longer polymer $E_{224}B_{113}$, the lamellar microdomains in the upper polymer layers exhibit mixed orientations of parallel and perpendicular to the surface. In the first half polymer layer contacting mica the stems of the E crystals

are parallel to the mica surface in all the E_mB_n thin films whereas the upper layers have a perpendicular orientation. Annealing leads to the formation of a half-layered, densely branched structure for thin films of all E_mB_n block copolymers on mica, in contrast to the featureless half-layered structure on silicon. During annealing, the polymers in the upper layers migrate to the bottom layer and the upper layers disappear gradually. The thickness of the upper polymer layers becomes larger but the thickness of the first half polymer contacting mica becomes smaller upon annealing. In both the cases the reason for this is lamellar thickening. In the first half layer where the stems are parallel to mica lamellar thickening leads to spreading and half-layer thinning whereas in the upper layer the islands contact but get thicker. The densely branched structure and the different chain orientation of the E crystal stems in the first half polymer layer contacting mica are attributed to the strong interaction between the E block and mica. It is also found that the width of the branches and the velocity of crystal front decrease as the chain length increases.

Acknowledgements

This research was supported by ICI and the National Natural Science Foundation of China (20374046 and 20674073), the Excellent Young Teachers Program and New Century Supporting Program for the Talents by the Chinese Ministry of Education.

References

[1] Fasolka MJ, Mayes AM. Annu Rev Mater Res 2001;31:323.
[2] Green PF, Limary R. Adv Colloid Interface Sci 2001;94:53.
[3] Segalman RA. Mater Sci Eng R 2005;48:191.
[4] Green PF. J Polym Sci Part B Polym Phys 2003;41:2219.
[5] Park C, Simmons S, Fetters LJ, Hsiao B, Yeh F, Thomas EL. Polymer 2000;41:2971.
[6] Daoulas KC, Muller M, Stoykovich MP, Park SM, Papakonstantopoulos YJ, de Pablo JJ, et al. Phys Rev Lett 2006:96.
[7] Aizawa M, Buriak JM. J Am Chem Soc 2006;128:5877.
[8] Yoon J, Lee W, Thomas EL. MRS Bull 2005;30:721.
[9] Yeh SW, Wu TL, Wei KH. Nanotechnology 2005;16:683.
[10] Wang Q. Macromol Theory Simul 2005;14:96.
[11] Ho RM, Tseng WH, Fan HW, Chiang YW, Lin CC, Ko BT, et al. Polymer 2005;46:9362.
[12] Peng J, Xuan Y, Wang HF, Yang YM, Li BY, Han YC. J Chem Phys 2004;120:11163.
[13] Edwards EW, Montague MF, Solak HH, Hawker CJ, Nealey PF. Adv Mater 2004;16:1315.
[14] Cheng JY, Mayes AM, Ross CA. Nat Mater 2004;3:823.
[15] Cheng JY, Jung W, Ross CA. Phys Rev B 2004:70.
[16] Cheng JY, Ross CA, Thomas EL, Smith HI, Vancso GJ. Adv Mater 2003;15:1599.
[17] Cheng JY, Ross CA, Thomas EL, Smith HI, Vancso GJ. Appl Phys Lett 2002;81:3657.
[18] Park M, Chaikin PM, Register RA, Adamson DH. Appl Phys Lett 2001;79:257.
[19] Park C, De Rosa C, Thomas EL. Macromolecules 2001;34:2602.
[20] Li RR, Dapkus PD, Thompson ME, Jeong WG, Harrison C, Chaikin PM, et al. Appl Phys Lett 2000;76:1689.
[21] Harrison C, Adamson DH, Cheng ZD, Sebastian JM, Sethuraman S, Huse DA, et al. Science 2000;290:1558.
[22] De Rosa C, Park C, Thomas EL, Lotz B. Nature 2000;405:433.
[23] Park M, Harrison C, Chaikin PM, Register RA, Adamson DH. Science 1997;276:1401.
[24] Ashok B, Muthukumar M, Russell TP. J Chem Phys 2001;115:1559.
[25] Waltman RJ, Khurshudov A, Tyndall GW. Tribol Lett 2002;12:163.
[26] Waltman RJ. Langmuir 2004;20:3166.
[27] Elhadj S, Woody JW, Niu VS, Saraf RF. Appl Phys Lett 2003;82:871.
[28] Reiter G, Khanna R, Sharma A. J Phys Condens Matter 2003;15:S331.
[29] Lee SH, Kang HM, Kim YS, Char K. Macromolecules 2003;36:4907.
[30] Harrison C, Cheng ZD, Sethuraman S, Huse DA, Chaikin PM, Vega DA, et al. Phys Rev E 2002:66.
[31] Xu T, Zhu YQ, Gido SP, Russell TP. Macromolecules 2004;37:2625.
[32] Segalman RA, Hexemer A, Hayward RC, Kramer EJ. Macromolecules 2003;36:3272.
[33] Segalman RA, Hexemer A, Kramer EJ. Phys Rev Lett 2003:91.
[34] Segalman RA, Hexemer A, Kramer EJ. Macromolecules 2003;36:6831.
[35] Segalman RA, Schaefer KE, Fredrickson GH, Kramer EJ, Magonov S. Macromolecules 2003;36:4498.
[36] Zhai XM, Wang W, Zhang GL, He BL. Macromolecules 2006;39:324.
[37] Loo YL, Register RA, Ryan AJ. Macromolecules 2002;35:2365.
[38] Xu JT, Fairclough JPA, Mai SM, Ryan AJ, Chaibundit C. Macromolecules 2002;35:6937.
[39] Li LB, Serero Y, Koch MHJ, de Jeu WH. Macromolecules 2003;36:529.
[40] Li LB, Lambreva D, de Jeu WH. J Macromol Sci Phys 2004;B43:59.
[41] Mansky P, Liu Y, Huang E, Russell TP, Hawker C. Science 1997;275:1458.
[42] Mansky P, Russell TP, Hawker CJ, Mays J, Cook DC, Satija SK. Phys Rev Lett 1997;79:237.
[43] Huang E, Russell TP, Harrison C, Chaikin PM, Register RA, Hawker CJ, et al. Macromolecules 1998;31:7641.
[44] Huang E, Rockford L, Russell TP, Hawker CJ. Nature 1998;395:757.
[45] Huang E, Pruzinsky S, Russell TP, Mays J, Hawker CJ. Macromolecules 1999;32:5299.
[46] Costa AC, Composto RJ, Vlcek P. Macromolecules 2003;36:3254.
[47] Liang GD, Xu JT, Fan ZQ, Mai SM, Ryan AJ. J Phys Chem B 2006;110:24384.
[48] Mai SM, Fairclough JPA, Viras K, Gorry PA, Hamley IW, Ryan AJ, et al. Macromolecules 1997;30:8392.
[49] Mai SM, Fairclough JPA, Terrill NJ, Turner SC, Hamley IW, Matsen MW, et al. Macromolecules 1998;31:8110.
[50] Ryan AJ, Mai SM, Fairclough JPA, Hamley IW, Booth C. Phys Chem Chem Phys 2001;3:2961.
[51] Xu JT, Turner SC, Fairclough JPA, Mai SM, Ryan AJ, Chaibundit C, et al. Macromolecules 2002;35:3614.
[52] Liang GD, Xu JT, Fan ZQ, Mai SM, Ryan AJ. Macromolecules 2006;39:5471.
[53] Murthy NS, Bednarczyk C, Minor H. Polymer 2000;41:277.
[54] Durell M, Macdonald JE, Trolley D, Wehrum A, Jukes PC, Jones RAL, et al. Europhys Lett 2002;58:844.
[55] Lee B, Park I, Yoon J, Park S, Kim J, Kim KW, et al. Macromolecules 2005;38:4311.
[56] Chen DJ, Gong YM, He TB, Zhang FJ. Macromolecules 2006;39:4101.
[57] Geke MO, Shelden RA, Caseri WR, Suter UW. J Colloid Interface Sci 1997;189:283.
[58] Surin M, Marsitzky D, Grimsdale AC, Mullen K, Lazzaroni R, Leclere P. Adv Funct Mater 2004;14:708.
[59] Chai L, Klein J. J Am Chem Soc 2005;127:1104.
[60] Reiter G, Sommer JU. Phys Rev Lett 1998;80:3771.
[61] Wang MT, Braun HG, Meyer E. Macromolecules 2004;37:437.
[62] Witten TA, Sander LM. Phys Rev Lett 1981;47:1400.
[63] Witten TA, Sander LM. Phys Rev B 1983;27:5686.
[64] Kovacs AJ, Gonthier A. Kolloid Z Z Polym 1972;250:530.
[65] Goldenfeld N. J Cryst Growth 1987;84:601.
[66] Brener E, Muller-Krumbhaar H, Temkin D. Phys Rev E 1996;54:2714.
[67] De Gennes PG. Scaling concepts in polymer physics. Ithaca: Cornell University Press; 1979.